Note

Understanding ATLAS track resolution with IDres.

The program IDres calculates the error matrix of tracking detectors with magnetic fields. It is useful for getting a rough idea very quickly of how well an inner tracker layout will perform. It is interesting to see how the resolution prediction from IDres compares to that from full-simulation with Geant4. For this, the ATLAS Inner Detector layout has been modelled and the resolution predictions are compared to the predictions published in the ATLAS Detector-Performance note ("CSC Book").

Prepared by:	*Checked by:*	*Approved by:*
N.P. Hessey	**Nobody**	**Nobody**

Distribution List:
Public

History of Changes

Rev. No.	Date	Pages	Made by	Description of changes
A	10/05/2010	All	N.P. Hessey	Original document
B		Most	N.P. Hessey	With variable B-field

Contents

1 Introduction

The program IDres [1] calculates the track covariance-matrix for inner trackers with approximately solenoidal fields. It is based on the method given in [2], which takes into account the hits with their resolutions and multiple scattering in layers. It was written to help guide designs for the ATLAS Inner Tracker replacement for the sLHC, but is very general with a simple ascii data file used to describe layouts.

It is useful to know how good IDres is at predicting track resolution. One way to do this is to test it on an inner tracker with known performance. The publication of two ATLAS notes simplifies this: there is sufficient detail on the ATLAS Inner Detector (ID) layout, including material distribution, in the ATLAS detector paper [3]; and detailed predictions of the ID performance in the ATLAS CSC note [4], based on detailed simulation with Athena/GEANT4. IDres makes many approximations so it is important to check it makes meaningful predictions. While IDres gives no information on track finding efficiency or fake rates, it is useful because it is fast: simple layouts can be constructed in a matter of hours, and the program takes about a minute to run, covering a wide range of track momenta and directions.

The results shown in this study demonstrate good agreement, suggesting in particular that IDres can be trusted to predict adequately the change in resolution to be expected in going from one layout to another similar one. This study was also a good check for bugs in the code, with a reasonably sophisticated geometry model built up.

Having developed an IDres geometry describing the ATLAS ID, it should be straightforward to add modifications to it to see how small changes in the ID will affect performance: e.g. adding the IBL or silicon discs in place of the staged TRT C-wheels; and the effects of losing a layer or a degraded resolution due to aging.

In the original version of this document a perfect solenoid B-field of 1.9 T was assumed. Since then, IDres has been improved to allow a magnetic field to be given numerically on an (r,z) grid, with axial and radial (B_z and B_r) components. IDres now carries out the double B-field integrals discussed in [2].

2 Layout

IDres geometries can involve cylinders and discs (and cones, but these are not used here), which are described by giving their positions in the two dimensions r and z. Each element also has hit resolutions in $r\phi$ and in the second coordinate (z in cylinders and r in discs) and a radiation length (in %X0).

At first a solenoidal B-field of 1.9 Tesla was assumed. The peak in the ID is 1.96 Tesla, while the value used here is representive over a large region of the ID. In fact, the ATLAS solenoid field is highly inhomogenous at the ends of the cryostat, and so a more realistic field, with both axial and radial components, and dependent on position, has now been modelled. The field was taken from early work (February 2006) by Steve Snow [6], file `sumne.grid`. This field is calculated for circular coils (when actually they are helical) and kept symmetric in ϕ and z; probably without the best magnetic material content. It has a maximum field in the cryostat volume of 2.00 T. Of course it would be even better to take the most up to date B-field map, but this field map was much easier to get started with than trying to dig out the full Atlas field map.

The layout used here was built up in stages: first the active layers (pixel, SCT, and TRT) were created. Then inactive layers were added to represent the supports and services which contribute

to multiple scattering. In IDres, inactive layers are the same as active ones but given a very bad resolution (like 1 km) so they give no useful measurement.

The resulting geometry file is included in appendix A and available at [5]. It is shown in figure 1, and can be compared to the detector paper geometry in figure 2. A second geometry file using the non-solenoidal field was identical except the 1.9 T value was replaced by the filenames for the variable B-field, and the following line added,

```
bIntegral 101 0.0 1.2 101 0.0 1.570793
```

to define the B-integration: 101 steps in both r and θ, covering zero to 1.2 m in r and zero to 90 degrees in θ.

2.1 Position-sensitive layers

Pixels and strips were straightforward to implement. Positions, resolutions and radiation lengths were taken from the detector paper. The radiation lengths in some cases were adjusted slightly to improve agreement with the material distribution plot.

The TRT consists of many straws with significant gaps between them. So instead of entering all layers, which would give too many hits, the layout models 36 layers in the barrel region – this is the typical number of hits. For the end-caps, the A and B wheels were modelled separately. There are 12 modules with 8 layers in each in the A wheels; These 96 layers were modelled as 48 discs, equispaced to fill the A-wheel region. There are 8 modules of 8 layers in the B-wheels; these were modelled as 32 equispaced layers.

Table 1 gives the resolutions used in the geometry file.

Sub-system	Precision coordinate	Second coordinate
Pixel	10	115
SCT	17	580
TRT	130	None (1 m)

Table 1: Hit resolutions (in microns) assumed in the different detector elements.

2.2 Inactive material (services)

Inert cylinders and discs were then added to represent mechanical supports and services. The geantino hit-map shown in figure 3 was used as a guide to decide where best to add elements.

No attempt was made to model material outside the tracking region $|\eta| > 2.5$. Material outside the last detector layer has no effect on track resolution, but was added anyway to simplify comparison of the material distributions between IDres and the detector paper.

The geometry was built up in separate stages for pixels, SCT, TRT, and finally the outermost services. This allows the amount of material to be adjusted in each inactive layer to give reasonable agreement.

This adjustment was made with guidance from the geantino hit map, statements in the detector paper, and trial and error. It does not come up with a unique, correct solution, but does end with reasonable agreement as seen in figure 4. In any case, in typical uses of IDres, the material distribution will not be well known.

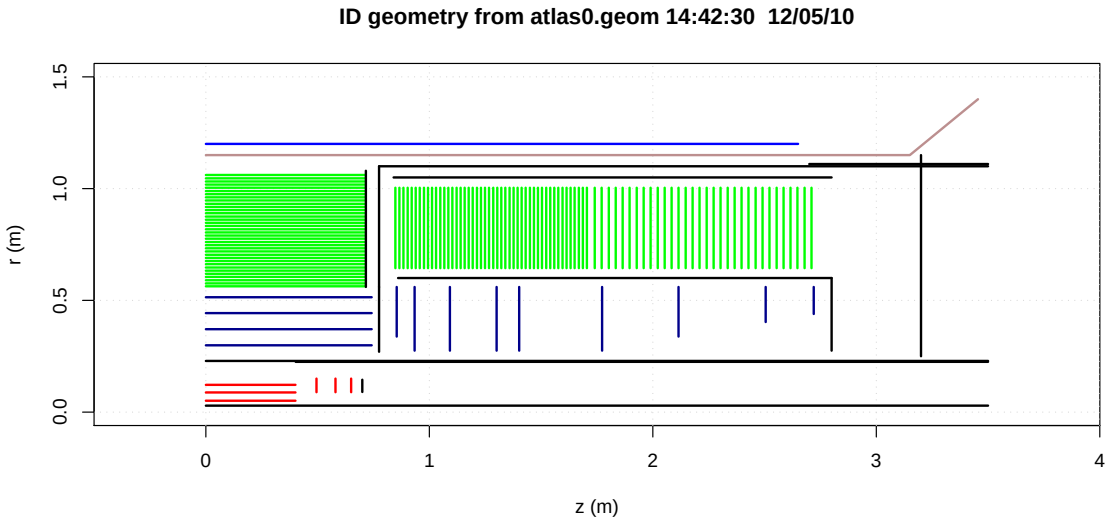

Figure 1: IDres geometry. Pixels, strips, TRT and inactive elements are red, dark blue, green, and black respectively.

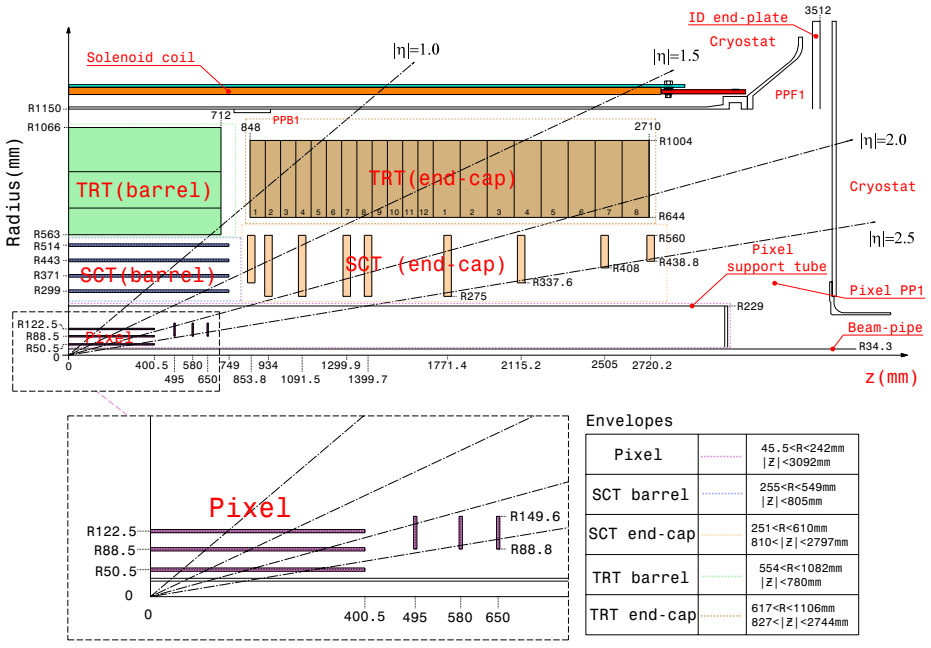

Figure 2: Detector paper geometry.

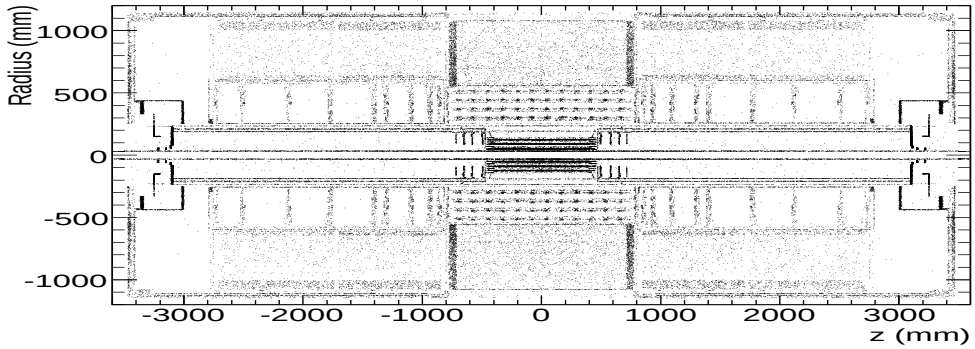

Figure 3: Detector paper geantino hit map.

3 Results

The resolutions for the five track parameters $(p_T, d_0, z_0, \cot\theta, \phi)$ have been calculated for track momenta of 1, 5, and 100 GeV/c to match the values used in the CSC note. η was varied from 0 to 2.5 in a large number of steps (250) making the IDres plots look continuous.

Figure 5 shows the IDres p_T resolution alongside the CSC-note prediction. The shapes are well reproduced. At low momentum, there is good agreement in magnitude everywhere. At 100 GeV/c and $\eta = 0$, IDres is optimistic at 0.33 compared with 0.39 in the CSC note, while at larger eta the agreement is again very good. IDres with a constant B-field is also optimistic for low-p_T tracks at high η (e.g. for 1 GeV/c tracks at $\eta = 2.5$ IDres predicts 4 % while the CSC-note gives 6 %). Taking into account the degradation in the field quality at high z improves the agreement significantly (but not fully). With the realistic B-field, the agreement is better than 20 % everywhere.

The IDres plot has sharper features than the CSC note reults. This comes from two effects: the CSC note averages over large η-bins (0.25 wide) while IDres calculates at discrete values (every 0.01); and the CSC prediction averages over a range of interaction points along z to simulate the expected spread of interactions in the LHC while IDres looks only at $z = 0$.

Figure 6 shows the d_0 results. Again, the shapes are well reproduced, IDres tends to be optimistic, and the agreement is typically within 10 %.

Figure 7 shows the $z_0 \sin\theta$ ("modified z_0 resolution") results. There is reasonable agreement at $\eta = 0$ and this continues to around $\eta = 1$. But after that, the predictions diverge, with IDres much more optimistic. For low momenta, at least the resolution starts to worsen again, but only reaching about 290 μminstead of 430 μmat $\eta = 2.5$. At higher momenta, IDres wrongly predicts continuous improvement with η. The cause of this has been partially investigated:

- The CSC note gives the error in $(z_0 \sin\theta)$ while for IDres, the plot shows $\sin\theta x($ error in $z_0)$. IDres assumes all tracks come from $z = 0$, for which these quantities are identical ($z_0 \sin\theta = 0$ at $z_0 = 0$ independently of θ). The possibility that tracks originating away from the origin cause the discrepancy was investigated by plotting the error in $(z_0 \sin\theta)$ for tracks originating at $z = 50$ mm (roughly the rms spread in z of the interactions). The curves did not change significantly except at 1 GeV/c, where it still failed to improve improve the shape.

- One expects the error on $z_0 \sin\theta$ to be determined mostly by the first two pixel layers. The IDres geometry has a fixed resolution along the pixel barrels. However, in reality this is not

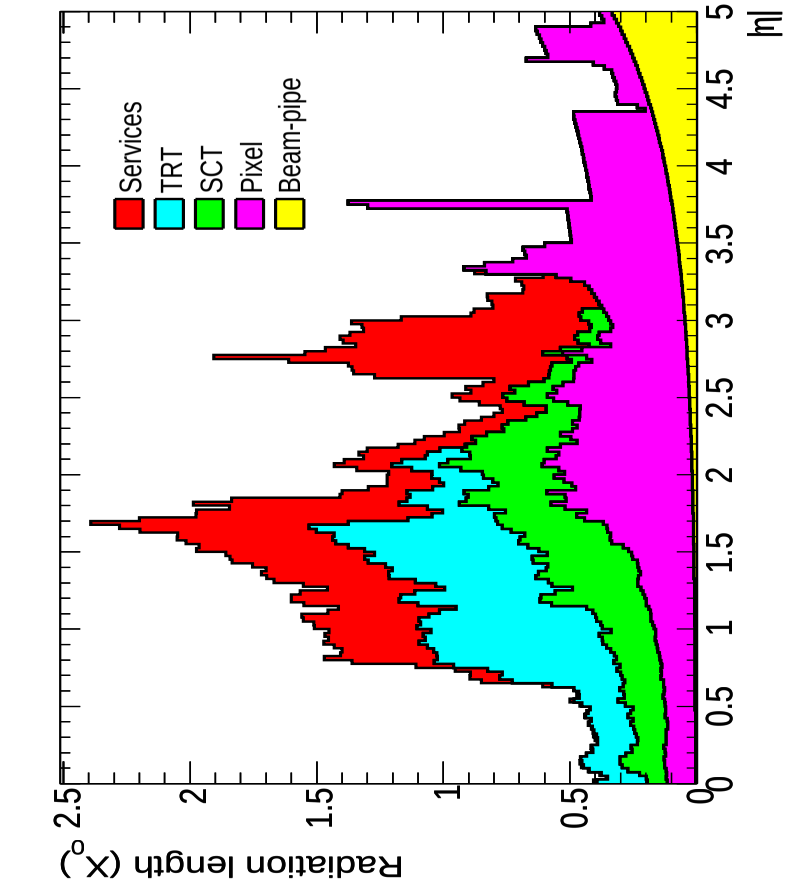

(b) Detector paper material

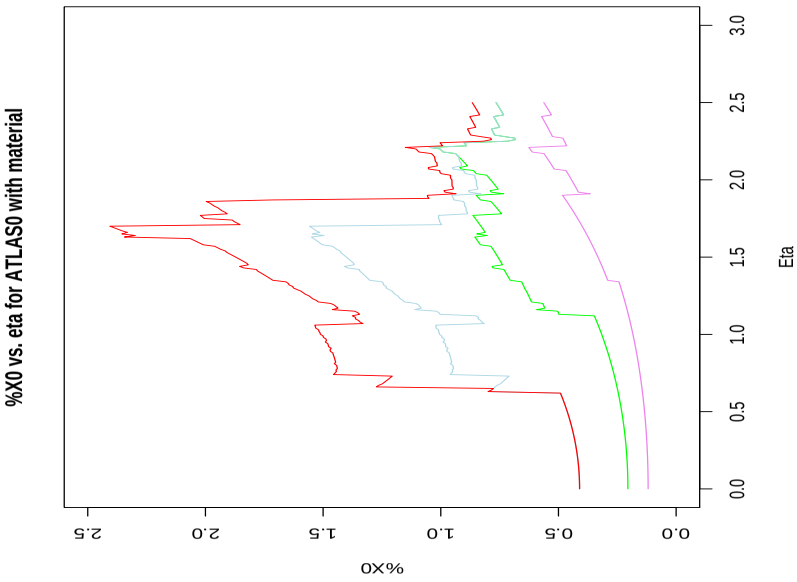

(a) IDres material distribution

Figure 4: Material distribution. Note the difference in eta ranges.

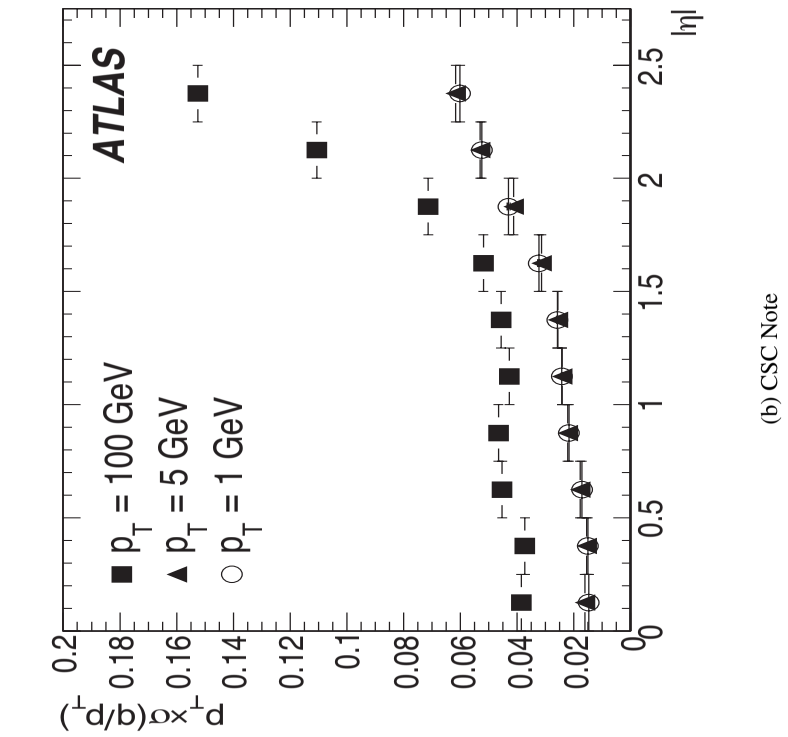

(b) CSC Note

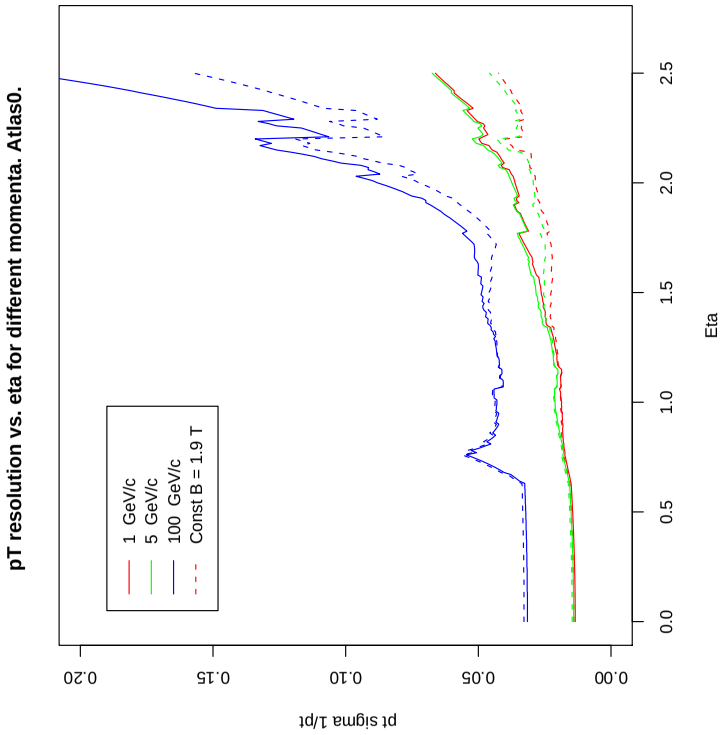

(a) IDres

Figure 5: Predicted p_T resolution as a function of η. Solid lines are for the detailed B-field map; dashed lines for the constant 1.9 T field. It is clearly important to use a realistic field at high η.

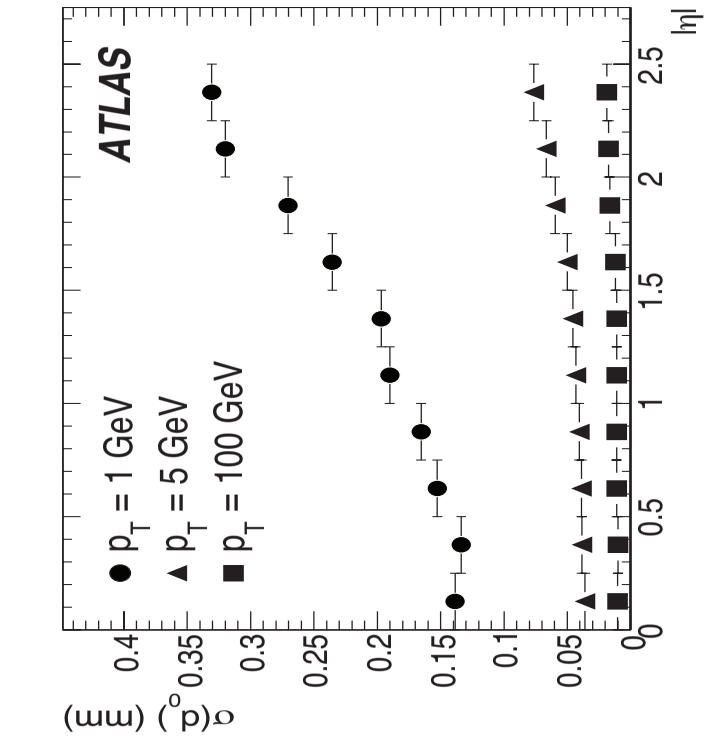

(b) CSC Note

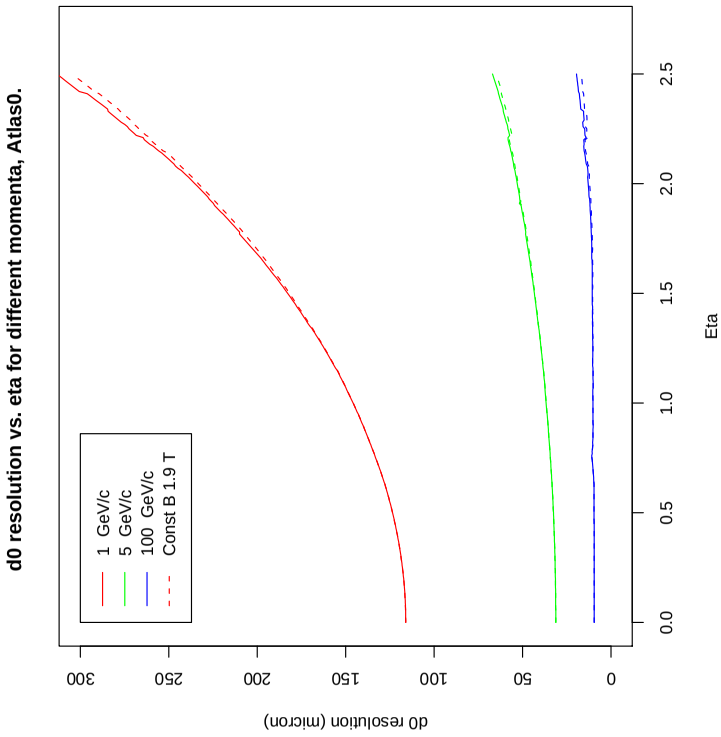

(a) IDres

Figure 6: Predicted d_0 resolution as a function of η.

the case. Forward going tracks cross many pixels in a row of fixed ϕ, making determination of the second-coordinate of the hit-centre difficult. The possibility that this contributes to the discrepancy was investigated by splitting the pixel barrel in z sections with deteriorating hit resolution as z increases. This significantly deteriorates the $z_0 \sin\theta$ resolution as *eta* increases, suggesting it could at least be part of the cause of the discrepancy. Further investigation of this is needed.

Figures 8 and 9 give the IDres predictions for $\cot\theta$ and ϕ. The CSC note does not give figures for comparison, giving merely the asymptotic values for infinite-momentum tracks at $\eta = 0$. For $\cot\theta$ this is 0.7×10^{-3}, comparing well with the IDres value for 100 GeV/c of 0.84×10^{-3}. Also for ϕ, the CSC value of 70 μrad compares well to the IDres value of 77 μrad.

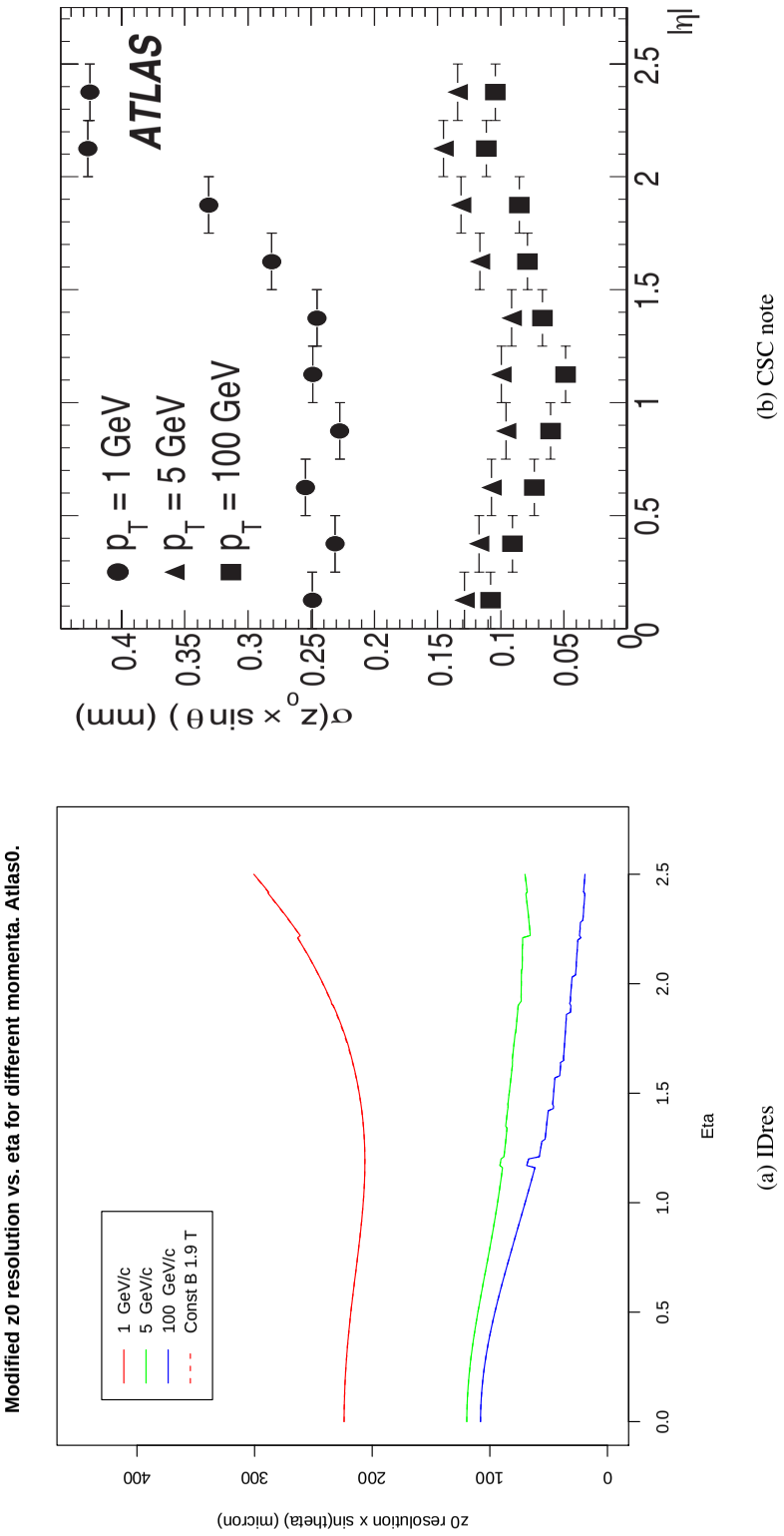

(b) CSC note

(a) IDres

Figure 7: Predicted z_0 resolution as a function of η.

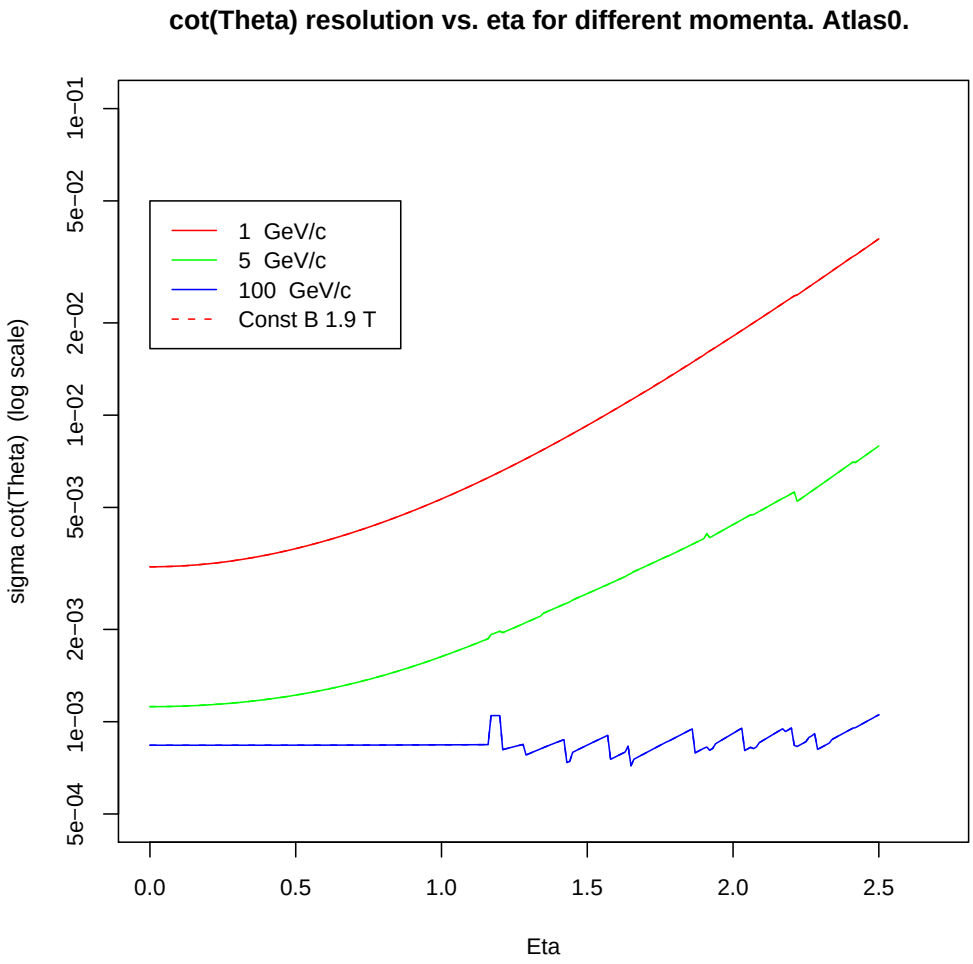

Figure 8: $\cot(\theta)$ resolution as a function of η predicted by IDres. The CSC note states the resolution tends to $0.7x10^{-3}$ for infinite momentum tracks at $\eta = 0$.

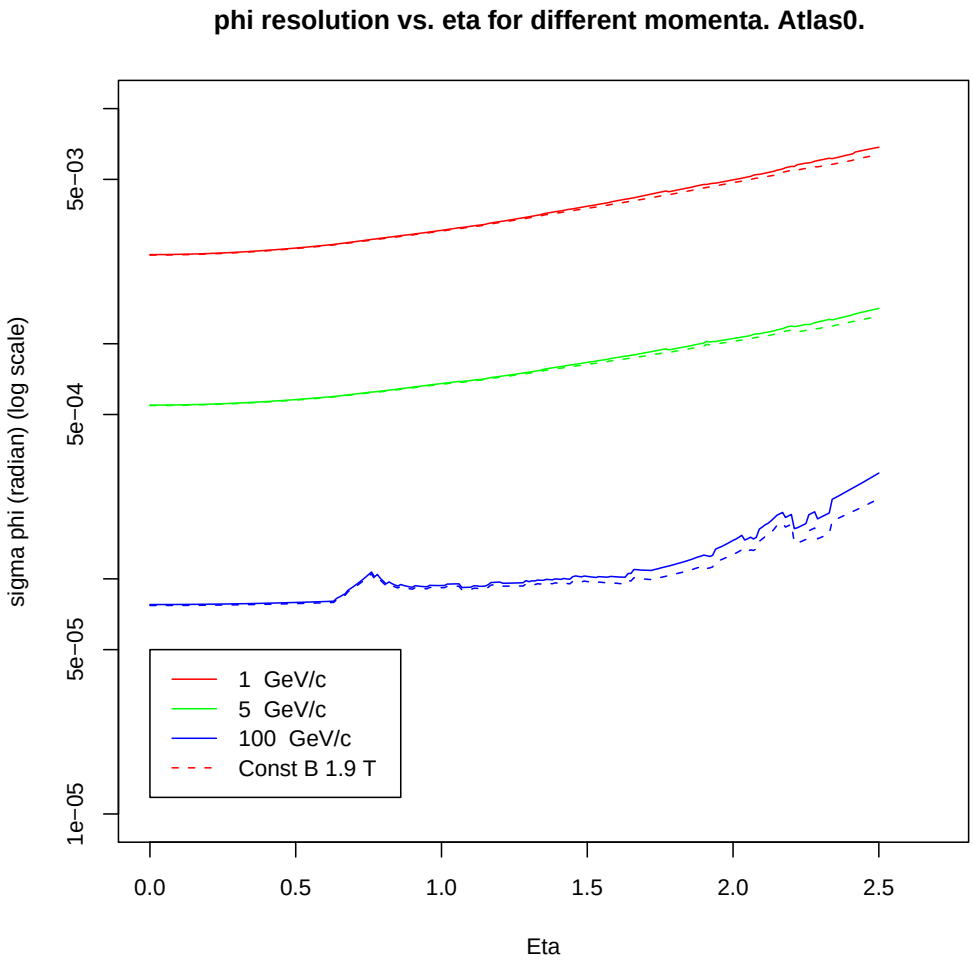

Figure 9: Phi resolution as a function of η predicted by IDres. The CSC note states the resolution tends to 70 μrad for infinite momentum tracks at $\eta = 0$.

4 Conclusion

The program IDres, with the geometry file developed here to model the ATLAS ID, gives very reasonable predictions for the track resolutions, typically well within 20 %. The prediction for $z_0 \sin\theta$ is less good, and deserves further investigation. The momentum resolution prediction at high-*eta* is considerably improved with a realistic B-field in place of assuming a constant solenoidal field.

This shows the ATLAS ID resolution can be well understood in terms of the B-field map, hit resolutions and multiple scattering in material.

The geometry file used here should make a good starting point for studies such as adding the IBL (a new b-layer), or extra silicon strip discs.

The results give good confidance in IDres as a tool to predict the tracking resolution of different proposed layouts for the sLHC inner tracker, especially for estimating differences between similar layouts.

5 Bibliography

References

[1] Introduction to IDres, N.P. Hessey, `http://www.nikhef.nl/~r29/upgrade/IDres.html`

[2] Parameterisation of the Inner Detector Performance by E-J Buis, R Dankers, A Reichold, S Haywood, 21 Jan 1998 - ATLAS Inner Detector note 97-195, available online at `http://preprints.cern.ch/cgi-bin/setlink?base=atlnot&categ=Note&id=indet-97-195`.

[3] The ATLAS Experiment at the CERN Large Hadron Collider, The ATLAS collaboration, available on-line at `http://iopscience.iop.org/1748-0221/3/08`.

[4] Expected Performance of the ATLAS Experiment - Detector, Trigger and Physics, The ATLAS Collaboration, available online at `http://cdsweb.cern.ch/record/1125884?ln=en`.

[5] The ascii geometry description used in these studies, given in the appendix, and available on-line at `http://www.nikhef.nl/~r29/upgrade/atlas0.geom`.

[6] S. Snow, B-field calculation results available on-line at `http://www.hep.man.ac.uk/u/miyagawa/work/bfield/output.html`. `sumne.grid` was used as the basis of this work.

A The geometry description used with IDres for this study

```
!
!    Atlas as-built geometry (loosely taken from ATLAS detector paper)
!
B 1.9 end

pt 1 5 100 end

eta
0.00  0.01  0.02  0.03  0.04  0.05  0.06  0.07  0.08  0.09  0.10  0.11  0.12  0.13  0.14  0.15
0.16  0.17  0.18  0.19  0.20  0.21  0.22  0.23  0.24  0.25  0.26  0.27  0.28  0.29  0.30  0.31
0.32  0.33  0.34  0.35  0.36  0.37  0.38  0.39  0.40  0.41  0.42  0.43  0.44  0.45  0.46  0.47
0.48  0.49  0.50  0.51  0.52  0.53  0.54  0.55  0.56  0.57  0.58  0.59  0.60  0.61  0.62  0.63
0.64  0.65  0.66  0.67  0.68  0.69  0.70  0.71  0.72  0.73  0.74  0.75  0.76  0.77  0.78  0.79
0.80  0.81  0.82  0.83  0.84  0.85  0.86  0.87  0.88  0.89  0.90  0.91  0.92  0.93  0.94  0.95
0.96  0.97  0.98  0.99  1.00  1.01  1.02  1.03  1.04  1.05  1.06  1.07  1.08  1.09  1.10  1.11
1.12  1.13  1.14  1.15  1.16  1.17  1.18  1.19  1.20  1.21  1.22  1.23  1.24  1.25  1.26  1.27
1.28  1.29  1.30  1.31  1.32  1.33  1.34  1.35  1.36  1.37  1.38  1.39  1.40  1.41  1.42  1.43
1.44  1.45  1.46  1.47  1.48  1.49  1.50  1.51  1.52  1.53  1.54  1.55  1.56  1.57  1.58  1.59
1.60  1.61  1.62  1.63  1.64  1.65  1.66  1.67  1.68  1.69  1.70  1.71  1.72  1.73  1.74  1.75
1.76  1.77  1.78  1.79  1.80  1.81  1.82  1.83  1.84  1.85  1.86  1.87  1.88  1.89  1.90  1.91
1.92  1.93  1.94  1.95  1.96  1.97  1.98  1.99  2.00  2.01  2.02  2.03  2.04  2.05  2.06  2.07
2.08  2.09  2.10  2.11  2.12  2.13  2.14  2.15  2.16  2.17  2.18  2.19  2.20  2.21  2.22  2.23
2.24  2.25  2.26  2.27  2.28  2.29  2.30  2.31  2.32  2.33  2.34  2.35  2.36  2.37  2.38  2.39
2.40  2.41  2.42  2.43  2.44  2.45  2.46  2.47  2.48  2.49  2.50
end

! Beam pipe
cylinder
    0.029 -3.5 3.5 0.45 1.e3 1.e3
end

! Pixels
cylinder
    0.0505  -0.4005  0.4005  3.25 10.0e-6  115e-6
    0.0885  -0.4005  0.4005  3.55 10.0e-6  115e-6
    0.1225  -0.4005  0.4005  3.55 10.0e-6  115e-6
end

! PST and services along it
cylinder
    0.229   -3.5  3.5   1.10 1.e3 1.e3
    0.225   -3.5 -0.402 2.22 1.e3 1.e3
    0.225   0.402 3.5   2.22 1.e3 1.e3
end

! Assume disc rad lens are 1.27 x cyl, like SCT (was 4.13)
disc
    0.0888  0.1496  0.495  4.5 10.0e-6 115e-6
    0.0888  0.1496  0.58   4.5 10.0e-6 115e-6
    0.0888  0.1496  0.65   4.5 10.0e-6 115e-6
end

disc
    0.0888  0.1496  -0.495  4.5 10.0e-6 115e-6
    0.0888  0.1496  -0.58   4.5 10.0e-6 115e-6
    0.0888  0.1496  -0.65   4.5 10.0e-6 115e-6
end
! Endwall Pixel:
disc
    0.09 0.145  0.7 4. 1.e3 1.e3
    0.09 0.145 -0.7 4. 1.e3 1.e3
end

! SCT.
cylinder
    0.2995  -0.7421  0.7421  2.15 17.0e-6 580e-6
```

```
    0.371   -0.7421  0.7421  2.15 17.0e-6 580e-6
    0.443   -0.7421  0.7421  2.15 17.0e-6 580e-6
    0.514   -0.7421  0.7421  2.15 17.0e-6 580e-6
end
! Services end-of-barrel
disc
    0.27 0.56  0.775 12. 1.e3 1.e3
    0.27 0.56 -0.775 12. 1.e3 1.e3
end
disc
    0.3376  0.56  0.8542  3.75 17.0e-6 580e-6
    0.275   0.56  0.9343  3.75 17.0e-6 580e-6
    0.275   0.56  1.0922  3.75 17.0e-6 580e-6
    0.275   0.56  1.3006  3.75 17.0e-6 580e-6
    0.275   0.56  1.4021  3.75 17.0e-6 580e-6
    0.275   0.56  1.7729  3.75 17.0e-6 580e-6
    0.3376  0.56  2.1147  3.75 17.0e-6 580e-6
    0.4028  0.56  2.5046  3.75 17.0e-6 580e-6
    0.4388  0.56  2.7198  3.75 17.0e-6 580e-6
end

disc
    0.3376  0.56  -0.8542  3.75 17.0e-6 580e-6
    0.275   0.56  -0.9343  3.75 17.0e-6 580e-6
    0.275   0.56  -1.0922  3.75 17.0e-6 580e-6
    0.275   0.56  -1.3006  3.75 17.0e-6 580e-6
    0.275   0.56  -1.4021  3.75 17.0e-6 580e-6
    0.275   0.56  -1.7729  3.75 17.0e-6 580e-6
    0.3376  0.56  -2.1147  3.75 17.0e-6 580e-6
    0.4028  0.56  -2.5046  3.75 17.0e-6 580e-6
    0.4388  0.56  -2.7198  3.75 17.0e-6 580e-6
end
! Services along SCT endcap
cylinder
    0.6  0.86 2.8  5.0 1.e3 1.e3
    0.6 -2.8 -0.86 5.0 1.e3 1.e3
end
! End-wall of endcap
disc
    0.275 0.6  2.8 5. 1.e3 1.e3
    0.275 0.6 -2.8 5. 1.e3 1.e3
end
! TRT Geomtry file. Add to pixel and SCT geometry files.

! TRT
cylinder
    0.563    -0.714  0.714  0.570  130.0e-6 1.0
    0.576    -0.714  0.714  0.570  130.0e-6 1.0
    0.59025  -0.714  0.714  0.570  130.0e-6 1.0
    0.60451  -0.714  0.714  0.570  130.0e-6 1.0
    0.61877  -0.714  0.714  0.570  130.0e-6 1.0
    0.63302  -0.714  0.714  0.570  130.0e-6 1.0
    0.64728  -0.714  0.714  0.570  130.0e-6 1.0
    0.66154  -0.714  0.714  0.570  130.0e-6 1.0
    0.6758   -0.714  0.714  0.570  130.0e-6 1.0
    0.69005  -0.714  0.714  0.570  130.0e-6 1.0
    0.70431  -0.714  0.714  0.570  130.0e-6 1.0
    0.71857  -0.714  0.714  0.570  130.0e-6 1.0
    0.73282  -0.714  0.714  0.570  130.0e-6 1.0
    0.74708  -0.714  0.714  0.570  130.0e-6 1.0
    0.76134  -0.714  0.714  0.570  130.0e-6 1.0
    0.7756   -0.714  0.714  0.570  130.0e-6 1.0
    0.78985  -0.714  0.714  0.570  130.0e-6 1.0
    0.80411  -0.714  0.714  0.570  130.0e-6 1.0
    0.81837  -0.714  0.714  0.570  130.0e-6 1.0
    0.83262  -0.714  0.714  0.570  130.0e-6 1.0
```

```
    0.84688  -0.714  0.714  0.570  130.0e-6 1.0
    0.86114  -0.714  0.714  0.570  130.0e-6 1.0
    0.8754   -0.714  0.714  0.570  130.0e-6 1.0
    0.88965  -0.714  0.714  0.570  130.0e-6 1.0
    0.90391  -0.714  0.714  0.570  130.0e-6 1.0
    0.91817  -0.714  0.714  0.570  130.0e-6 1.0
    0.93242  -0.714  0.714  0.570  130.0e-6 1.0
    0.94668  -0.714  0.714  0.570  130.0e-6 1.0
    0.96094  -0.714  0.714  0.570  130.0e-6 1.0
    0.9752   -0.714  0.714  0.570  130.0e-6 1.0
    0.98945  -0.714  0.714  0.570  130.0e-6 1.0
    1.00371  -0.714  0.714  0.570  130.0e-6 1.0
    1.01797  -0.714  0.714  0.570  130.0e-6 1.0
    1.03223  -0.714  0.714  0.570  130.0e-6 1.0
    1.04649  -0.714  0.714  0.570  130.0e-6 1.0
    1.06074  -0.714  0.714  0.570  130.0e-6 1.0
end
! TRT Electronics
!    barrel:
disc
    0.56 1.08 -0.716 17 1.e3 1.e3
    0.56 1.08  0.716 17 1.e3 1.e3
end
!    endcap:
cylinder
    1.05  0.84  2.80 20 1.e3 1.e3
    1.05 -2.8  -0.84 20 1.e3 1.e3
end
! A-wheels, end A
disc
     0.644  1.004  0.848  0.490 130.0e-6 1.0
     0.644  1.004  0.866  0.490 130.0e-6 1.0
     0.644  1.004  0.884  0.490 130.0e-6 1.0
     0.644  1.004  0.903  0.490 130.0e-6 1.0
     0.644  1.004  0.921  0.490 130.0e-6 1.0
     0.644  1.004  0.939  0.490 130.0e-6 1.0
     0.644  1.004  0.957  0.490 130.0e-6 1.0
     0.644  1.004  0.976  0.490 130.0e-6 1.0
     0.644  1.004  0.994  0.490 130.0e-6 1.0
     0.644  1.004  1.012  0.490 130.0e-6 1.0
     0.644  1.004  1.030  0.490 130.0e-6 1.0
     0.644  1.004  1.049  0.490 130.0e-6 1.0
     0.644  1.004  1.067  0.490 130.0e-6 1.0
     0.644  1.004  1.085  0.490 130.0e-6 1.0
     0.644  1.004  1.103  0.490 130.0e-6 1.0
     0.644  1.004  1.122  0.490 130.0e-6 1.0
     0.644  1.004  1.140  0.490 130.0e-6 1.0
     0.644  1.004  1.158  0.490 130.0e-6 1.0
     0.644  1.004  1.176  0.490 130.0e-6 1.0
     0.644  1.004  1.194  0.490 130.0e-6 1.0
     0.644  1.004  1.213  0.490 130.0e-6 1.0
     0.644  1.004  1.231  0.490 130.0e-6 1.0
     0.644  1.004  1.249  0.490 130.0e-6 1.0
     0.644  1.004  1.267  0.490 130.0e-6 1.0
     0.644  1.004  1.286  0.490 130.0e-6 1.0
     0.644  1.004  1.304  0.490 130.0e-6 1.0
     0.644  1.004  1.322  0.490 130.0e-6 1.0
     0.644  1.004  1.340  0.490 130.0e-6 1.0
     0.644  1.004  1.359  0.490 130.0e-6 1.0
     0.644  1.004  1.377  0.490 130.0e-6 1.0
     0.644  1.004  1.395  0.490 130.0e-6 1.0
     0.644  1.004  1.413  0.490 130.0e-6 1.0
     0.644  1.004  1.431  0.490 130.0e-6 1.0
     0.644  1.004  1.450  0.490 130.0e-6 1.0
     0.644  1.004  1.468  0.490 130.0e-6 1.0
     0.644  1.004  1.486  0.490 130.0e-6 1.0
```

```
     0.644  1.004  1.504  0.490 130.0e-6 1.0
     0.644  1.004  1.523  0.490 130.0e-6 1.0
     0.644  1.004  1.541  0.490 130.0e-6 1.0
     0.644  1.004  1.559  0.490 130.0e-6 1.0
     0.644  1.004  1.577  0.490 130.0e-6 1.0
     0.644  1.004  1.596  0.490 130.0e-6 1.0
     0.644  1.004  1.614  0.490 130.0e-6 1.0
     0.644  1.004  1.632  0.490 130.0e-6 1.0
     0.644  1.004  1.650  0.490 130.0e-6 1.0
     0.644  1.004  1.669  0.490 130.0e-6 1.0
     0.644  1.004  1.687  0.490 130.0e-6 1.0
     0.644  1.004  1.705  0.490 130.0e-6 1.0
end
! A-wheels, end-C
disc
     0.644  1.004 -0.848  0.490 130.0e-6 1.0
     0.644  1.004 -0.866  0.490 130.0e-6 1.0
     0.644  1.004 -0.884  0.490 130.0e-6 1.0
     0.644  1.004 -0.903  0.490 130.0e-6 1.0
     0.644  1.004 -0.921  0.490 130.0e-6 1.0
     0.644  1.004 -0.939  0.490 130.0e-6 1.0
     0.644  1.004 -0.957  0.490 130.0e-6 1.0
     0.644  1.004 -0.976  0.490 130.0e-6 1.0
     0.644  1.004 -0.994  0.490 130.0e-6 1.0
     0.644  1.004 -1.012  0.490 130.0e-6 1.0
     0.644  1.004 -1.030  0.490 130.0e-6 1.0
     0.644  1.004 -1.049  0.490 130.0e-6 1.0
     0.644  1.004 -1.067  0.490 130.0e-6 1.0
     0.644  1.004 -1.085  0.490 130.0e-6 1.0
     0.644  1.004 -1.103  0.490 130.0e-6 1.0
     0.644  1.004 -1.122  0.490 130.0e-6 1.0
     0.644  1.004 -1.140  0.490 130.0e-6 1.0
     0.644  1.004 -1.158  0.490 130.0e-6 1.0
     0.644  1.004 -1.176  0.490 130.0e-6 1.0
     0.644  1.004 -1.194  0.490 130.0e-6 1.0
     0.644  1.004 -1.213  0.490 130.0e-6 1.0
     0.644  1.004 -1.231  0.490 130.0e-6 1.0
     0.644  1.004 -1.249  0.490 130.0e-6 1.0
     0.644  1.004 -1.267  0.490 130.0e-6 1.0
     0.644  1.004 -1.286  0.490 130.0e-6 1.0
     0.644  1.004 -1.304  0.490 130.0e-6 1.0
     0.644  1.004 -1.322  0.490 130.0e-6 1.0
     0.644  1.004 -1.340  0.490 130.0e-6 1.0
     0.644  1.004 -1.359  0.490 130.0e-6 1.0
     0.644  1.004 -1.377  0.490 130.0e-6 1.0
     0.644  1.004 -1.395  0.490 130.0e-6 1.0
     0.644  1.004 -1.413  0.490 130.0e-6 1.0
     0.644  1.004 -1.431  0.490 130.0e-6 1.0
     0.644  1.004 -1.450  0.490 130.0e-6 1.0
     0.644  1.004 -1.468  0.490 130.0e-6 1.0
     0.644  1.004 -1.486  0.490 130.0e-6 1.0
     0.644  1.004 -1.504  0.490 130.0e-6 1.0
     0.644  1.004 -1.523  0.490 130.0e-6 1.0
     0.644  1.004 -1.541  0.490 130.0e-6 1.0
     0.644  1.004 -1.559  0.490 130.0e-6 1.0
     0.644  1.004 -1.577  0.490 130.0e-6 1.0
     0.644  1.004 -1.596  0.490 130.0e-6 1.0
     0.644  1.004 -1.614  0.490 130.0e-6 1.0
     0.644  1.004 -1.632  0.490 130.0e-6 1.0
     0.644  1.004 -1.650  0.490 130.0e-6 1.0
     0.644  1.004 -1.669  0.490 130.0e-6 1.0
     0.644  1.004 -1.687  0.490 130.0e-6 1.0
     0.644  1.004 -1.705  0.490 130.0e-6 1.0
end
! B-wheels, end A
disc
```

```
     0.644  1.004  1.740  0.490 130.0e-6 1.0
     0.644  1.004  1.771  0.490 130.0e-6 1.0
     0.644  1.004  1.803  0.490 130.0e-6 1.0
     0.644  1.004  1.834  0.490 130.0e-6 1.0
     0.644  1.004  1.865  0.490 130.0e-6 1.0
     0.644  1.004  1.896  0.490 130.0e-6 1.0
     0.644  1.004  1.928  0.490 130.0e-6 1.0
     0.644  1.004  1.959  0.490 130.0e-6 1.0
     0.644  1.004  1.990  0.490 130.0e-6 1.0
     0.644  1.004  2.022  0.490 130.0e-6 1.0
     0.644  1.004  2.053  0.490 130.0e-6 1.0
     0.644  1.004  2.084  0.490 130.0e-6 1.0
     0.644  1.004  2.115  0.490 130.0e-6 1.0
     0.644  1.004  2.147  0.490 130.0e-6 1.0
     0.644  1.004  2.178  0.490 130.0e-6 1.0
     0.644  1.004  2.209  0.490 130.0e-6 1.0
     0.644  1.004  2.241  0.490 130.0e-6 1.0
     0.644  1.004  2.272  0.490 130.0e-6 1.0
     0.644  1.004  2.303  0.490 130.0e-6 1.0
     0.644  1.004  2.335  0.490 130.0e-6 1.0
     0.644  1.004  2.366  0.490 130.0e-6 1.0
     0.644  1.004  2.397  0.490 130.0e-6 1.0
     0.644  1.004  2.428  0.490 130.0e-6 1.0
     0.644  1.004  2.460  0.490 130.0e-6 1.0
     0.644  1.004  2.491  0.490 130.0e-6 1.0
     0.644  1.004  2.522  0.490 130.0e-6 1.0
     0.644  1.004  2.554  0.490 130.0e-6 1.0
     0.644  1.004  2.585  0.490 130.0e-6 1.0
     0.644  1.004  2.616  0.490 130.0e-6 1.0
     0.644  1.004  2.647  0.490 130.0e-6 1.0
     0.644  1.004  2.679  0.490 130.0e-6 1.0
     0.644  1.004  2.710  0.490 130.0e-6 1.0
end
! B-wheels, end C
disc
     0.644  1.004 -1.740  0.490 130.0e-6 1.0
     0.644  1.004 -1.771  0.490 130.0e-6 1.0
     0.644  1.004 -1.803  0.490 130.0e-6 1.0
     0.644  1.004 -1.834  0.490 130.0e-6 1.0
     0.644  1.004 -1.865  0.490 130.0e-6 1.0
     0.644  1.004 -1.896  0.490 130.0e-6 1.0
     0.644  1.004 -1.928  0.490 130.0e-6 1.0
     0.644  1.004 -1.959  0.490 130.0e-6 1.0
     0.644  1.004 -1.990  0.490 130.0e-6 1.0
     0.644  1.004 -2.022  0.490 130.0e-6 1.0
     0.644  1.004 -2.053  0.490 130.0e-6 1.0
     0.644  1.004 -2.084  0.490 130.0e-6 1.0
     0.644  1.004 -2.115  0.490 130.0e-6 1.0
     0.644  1.004 -2.147  0.490 130.0e-6 1.0
     0.644  1.004 -2.178  0.490 130.0e-6 1.0
     0.644  1.004 -2.209  0.490 130.0e-6 1.0
     0.644  1.004 -2.241  0.490 130.0e-6 1.0
     0.644  1.004 -2.272  0.490 130.0e-6 1.0
     0.644  1.004 -2.303  0.490 130.0e-6 1.0
     0.644  1.004 -2.335  0.490 130.0e-6 1.0
     0.644  1.004 -2.366  0.490 130.0e-6 1.0
     0.644  1.004 -2.397  0.490 130.0e-6 1.0
     0.644  1.004 -2.428  0.490 130.0e-6 1.0
     0.644  1.004 -2.460  0.490 130.0e-6 1.0
     0.644  1.004 -2.491  0.490 130.0e-6 1.0
     0.644  1.004 -2.522  0.490 130.0e-6 1.0
     0.644  1.004 -2.554  0.490 130.0e-6 1.0
     0.644  1.004 -2.585  0.490 130.0e-6 1.0
     0.644  1.004 -2.616  0.490 130.0e-6 1.0
     0.644  1.004 -2.647  0.490 130.0e-6 1.0
     0.644  1.004 -2.679  0.490 130.0e-6 1.0
```

```
     0.644  1.004 -2.710  0.490 130.0e-6 1.0
end


! Add to pixel, sct and trt to get whole ID
! Services along barrel end
disc
    0.56 1.10  0.775 15 1.e3 1.e3
    0.56 1.10 -0.775 15 1.e3 1.e3
end
! Services along cryostat wall (To get agreement with detector paper, no effect on
!performance)
cylinder
    1.10 -3.5 -0.775 20 1.e3 1.e3
    1.10  0.775  3.5 20 1.e3 1.e3
    1.11   2.7  3.5 10 1.e3 1.e3
    1.11  -3.5 -2.7 10 1.e3 1.e3
end
! Pixel services at end of cryostat
disc
   0.25 1.15  3.2 10 1.e3 1.e3
   0.25 1.15 -3.2 10 1.e3 1.e3
end
```